

# Zn-doping effect on the magnetotransport properties of $\text{Bi}_2\text{Sr}_{2-x}\text{La}_x\text{CuO}_{6+\delta}$ single crystals

Y. Hanaki<sup>1,2,\*</sup>, Yoichi Ando<sup>1,2,†</sup>, S. Ono<sup>1</sup>, and J. Takeya<sup>1</sup>

<sup>1</sup>*Central Research Institute of Electric Power Industry, Komae, Tokyo 201-8511, Japan*

<sup>2</sup>*Department of Physics, Science University of Tokyo, Shinjuku-ku, Tokyo 162-8601, Japan*  
(May 20, 2019)

We report the magnetotransport properties of  $\text{Bi}_2\text{Sr}_{2-x}\text{La}_x\text{Cu}_{1-z}\text{Zn}_z\text{O}_{6+\delta}$  (Zn-doped BSLCO) single crystals with  $z$  of up to 2.2%. Besides the typical Zn-doping effects on the in-plane resistivity and the Hall angle, we demonstrate that the nature of the low-temperature normal state in the Zn-doped samples is significantly altered from that in the pristine samples under high magnetic fields. In particular, we observe nearly-isotropic negative magnetoresistance as well as an increase in the Hall coefficient at very low temperatures in non-superconducting Zn-doped samples, which we propose to be caused by the Kondo scattering from the local moments induced by Zn impurities.

PACS numbers: 74.25.Fy, 74.62.Dh, 74.20.Mn, 74.72.Hs

Effects of nonmagnetic Zn impurities on the electronic properties of the high- $T_c$  cuprates have been intensively studied, employing almost all available experimental tools. However, well-controlled studies of the Zn-doping effects using high-quality single crystals have been mostly limited to the  $\text{YBa}_2\text{Cu}_3\text{O}_{7-\delta}$  (YBCO) system and the  $\text{La}_{2-x}\text{Sr}_x\text{CuO}_4$  (LSCO) system because of the availability of single crystals; for example, in the otherwise well-studied system of  $\text{Bi}_2\text{Sr}_2\text{CaCu}_2\text{O}_{8+\delta}$  (Bi-2212), high-quality single crystals can be grown with only up to  $\sim 1\%$  of Zn substitution, posing difficulties for systematic studies. Recently, high-quality single crystals of  $\text{Bi}_2\text{Sr}_{2-x}\text{La}_x\text{CuO}_{6+\delta}$  (BSLCO) have become available<sup>1</sup> in a wide range of hole concentrations.<sup>2</sup> It is thus natural to investigate the Zn-doping effect in the BSLCO system to examine and expand our knowledge of the role of Zn impurities in the cuprates. Here we report that Zn-doping of up to 2.2% is possible in high-quality BSLCO crystals and present the effect of Zn impurities on the charge transport properties of this system.

One of the most peculiar charge transport properties of the cuprates is that two distinct scattering rates,  $\tau_{tr}^{-1}$  and  $\tau_H^{-1}$ , possibly govern the in-plane resistivity  $\rho_{ab}$  and the Hall angle  $\theta_H$ , respectively. Zn impurities have been believed to induce<sup>3,4</sup> residual terms in both  $\tau_{tr}^{-1}$  and  $\tau_H^{-1}$ , which ultimately lead to charge localization<sup>5</sup>; these residual scattering rates may well be related<sup>6</sup> to the local moments induced by the nonmagnetic Zn impurities,<sup>7</sup> though the role of the local moments in the charge transport in cuprates is not well understood yet. It would thus be meaningful to look for some peculiar features that is clearly due to the local moments in the transport properties of the Zn-doped BSLCO crystals.

Perhaps the best-known effect of Zn-doping in cuprates is the rapid suppression of  $T_c$ . The rate of  $T_c$  suppression has been known to be around 10–15 K/at.% upon Zn substitution. It has been suggested<sup>8,9</sup> that this rate can be enhanced to  $\sim 20$  K/at.% near the hole concentration per Cu,  $p$ , of  $1/8$ , which was discussed to be due to the “pinning”<sup>10</sup> of the charge stripes<sup>11</sup> by Zn impuri-

ties. Since it was recently revealed<sup>12</sup> that the metal-to-insulator (M-I) crossover in the low-temperature normal state of BSLCO occurs at  $p \simeq 1/8$ , it is particularly intriguing to look at the effect of Zn at  $p \simeq 1/8$  to elucidate the impact of the charge-stripes instability in BSLCO.

In this paper, we report the charge transport properties in Zn-doped BSLCO ( $\text{Bi}_2\text{Sr}_{2-x}\text{La}_x\text{Cu}_{1-z}\text{Zn}_z\text{O}_{6+\delta}$ ) single crystals with  $z$  of up to 2.2% for  $x = 0.50$  and  $0.66$ . These La contents correspond to  $p$  of  $\sim 0.15$  and  $\sim 1/8$ , respectively,<sup>2</sup> and 2.2%-Zn is enough to completely suppress superconductivity at  $x = 0.66$ . We observe more or less standard Zn-doping effects in the in-plane resistivity, Hall angle, and  $T_c$ , without any noticeable “ $1/8$  anomaly” in the Zn-doped samples. On the other hand, we found very peculiar negative magnetoresistance as well as an upturn in  $R_H$  at low temperatures in non-superconducting samples, which is most likely to be related to the local moments induced by Zn.

The crystals are grown by a floating-zone technique as reported previously.<sup>1</sup> We have demonstrated<sup>1,2,12</sup> that our crystals are among the best available BSLCO crystals in terms of optimum  $T_c$  (which is as high as 38 K), residual resistivity, and the control of hole doping. The La concentrations in the crystals are determined by the electron-probe microanalysis (EPMA), and the actual Zn concentrations are measured by the inductively-coupled plasma (ICP) analysis; the errors in  $x$  and  $z$  are estimated to be  $\pm 0.01$  and  $\pm 0.002$ , respectively. For the transport measurements, the crystals are cut into dimensions typically  $1 \times 0.5 \times 0.02$  mm<sup>3</sup>. The thickness of the samples are calculated from their weight (measured with  $0.1\text{-}\mu\text{g}$  resolution) to accurately determine the absolute values of  $\rho_{ab}$  and the Hall coefficient  $R_H$ . All the crystals are annealed in air at  $650^\circ\text{C}$  for 48 h and quenched to room temperature to achieve uniform oxygen distribution. A standard ac six-probe method is employed to measure  $\rho_{ab}$  and  $R_H$ . The magnetoresistance and  $R_H$  are measured by sweeping the magnetic field to both plus and minus polarities at constant temperatures.<sup>1</sup> For the non-superconducting samples with  $(x, z) = (0.66, 0.022)$ ,

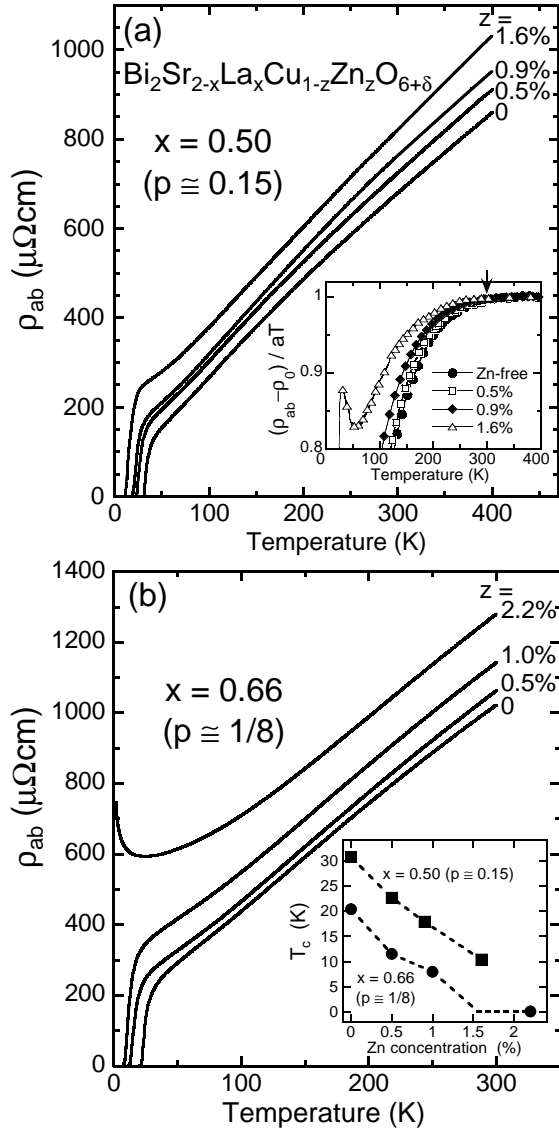


FIG. 1.  $\rho_{ab}(T)$  data of Bi<sub>2</sub>Sr<sub>2-x</sub>La<sub>x</sub>Cu<sub>1-z</sub>ZnO<sub>6+δ</sub> single crystals at (a)  $x = 0.50$  and (b)  $x = 0.66$  with various  $z$ . Inset to (a): Plots of  $(\rho_{ab} - \rho_0)/aT$  vs.  $T$  for  $x = 0.50$  with the four  $z$  values; arrow marks  $T^*$ . Inset to (b): Plots of  $T_c$  vs.  $z$  for  $x = 0.50$  and  $0.66$ .

we measure both the transverse and longitudinal magnetoresistance (MR) down to 450 mK in a <sup>3</sup>He refrigerator where the temperature control during the magnetic-field sweep is done with a stability of  $\sim 1$  mK using a capacitance sensor embedded in the sample stage.

Figures 1(a) and 1(b) show temperature dependences of  $\rho_{ab}$  for  $x = 0.50$  and  $0.66$  with various Zn concentrations. One can see that at both  $x$  the  $\rho_{ab}(T)$  curves are almost parallel-shifted upon Zn doping, indicating that the main effect of Zn impurities on  $\rho_{ab}$  is to increase a temperature-independent residual term in  $\tau_{tr}^{-1}$ . In the  $x = 0.50$  series [Fig. 1(a)], there is a reasonably wide region of  $T$ -linear resistivity at high temperatures, so that we can estimate the pseudogap temperature  $T^*$  for each Zn

concentration from the downward deviation of the  $\rho_{ab}(T)$  curves from the  $T$ -linear behavior. The inset of Fig. 1(a) shows the plots of  $[\rho_{ab}(T) - \rho_0]/aT$  vs.  $T$  (where  $a$  is the  $T$ -linear slope and  $\rho_0$  is the zero-temperature intercept of the  $T$ -linear behavior), which make it clear that the deviation takes place at nearly the same temperature ( $\sim 300$  K) for all  $z$ . Thus, as was reported<sup>13</sup> for YBCO,  $T^*$  as determined from  $\rho_{ab}(T)$  does not move with Zn doping in BSLCO.

In the  $x = 0.66$  series [Fig. 1(b)], it is notable that the superconductor-to-insulator (S-I) transition occurs around  $\rho_{ab}$  of  $\sim 400 \mu\Omega\text{cm}$ , which corresponds to the sheet resistance per CuO<sub>2</sub> plane of  $\sim 3.3 \text{ k}\Omega$ ; this is half the quantum value  $h/(2e)^2$  ( $\simeq 6.5 \text{ k}\Omega$ ) and thus differs by a factor of 2 from the result of the critical sheet resistance obtained<sup>4,13</sup> for YBCO and LSCO, indicating that the “universal” critical sheet resistance for the S-I transition is not exactly universal for the cuprates. We emphasize that the uncertainty in the absolute value of  $\rho_{ab}$  is less than 10% in our measurements.<sup>12</sup>

The inset of Fig. 1(b) shows the suppression of  $T_c$  upon Zn doping for the two  $x$  values; the suppression rates are almost the same for the two cases and is about 13 K/at.%, which is typical for the cuprates. Note that there is no enhancement in the  $T_c$ -suppression rate for  $p \simeq 1/8$  ( $x = 0.66$ ), and thus the sort of amplification of the  $1/8$  anomaly suggested<sup>8,9</sup> for LSCO and Bi-2212 are not observed in BSLCO. This can be interpreted to mean that the charge-order instability at  $p \simeq 1/8$  is so weak<sup>14</sup> in BSLCO that the “pinning” by the Zn impurities are not effective, though this interpretation is highly speculative.

Figures 2(a) and 2(b) show the temperature dependences of  $R_H$  for the two series. For each  $x$ , the magnitude of  $R_H$  does not change with  $z$  above 200 K, demonstrating that the Zn substitution does not change the hole concentration. At lower temperatures,  $R_H$  becomes  $z$  dependent and the peak in  $R_H(T)$  shows a non-monotonic change upon Zn doping. As is the case with other systems, the complicated change in  $R_H(T)$  can be simplified by looking at the Hall angle. Figures 2(c) and 2(d) show the plots of  $\cot \theta_H$  vs.  $T^2$  for the two series. All the data of  $\cot \theta_H$  are almost linear in  $T^2$  and appear to be parallel-shifted upon Zn doping, suggesting that the Zn impurities increase a temperature-independent residual term in  $\tau_H^{-1}$ ; this is actually the behavior that led to the two-scattering-rate scenario<sup>3</sup> and thus is typical for the cuprates. Upon closer look at the data in Figs. 2(c) and 2(d), one may notice that at low temperatures there is an upward deviation from the  $T^2$  behavior in the Zn-doped samples. To make this point clear, Figs. 2(e) and 2(f) show the plots of  $(\cot \theta_H - c)/bT^2$  vs.  $T$ , where  $b$  is the  $T^2$  slope and  $c$  is the zero-temperature intercept of the linear-in- $T^2$  behavior. One can see that the deviation becomes systematically more pronounced as  $z$  is increased; this behavior most likely reflects some localization effect in the Hall channel and is probably responsible for the weakening of the temperature dependence of  $R_H$  upon

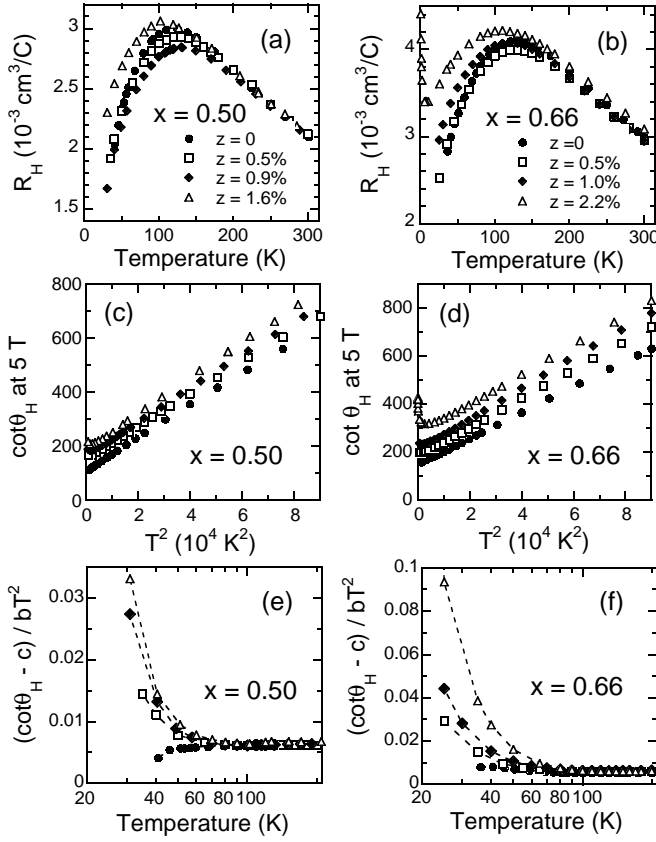


FIG. 2. (a),(b):  $T$  dependences of  $R_H$  for (a)  $x = 0.50$  and (b)  $x = 0.66$  with various  $z$ . (c),(d): Plots of  $\cot \theta_H$  vs.  $T^2$  for the two series. (e),(f): Plots of  $(\cot \theta_H - c)/bT^2$  vs.  $T$  for the two series, which emphasize the deviation from the  $T^2$  behavior.

#### Zn doping.

As already noted, the superconductivity is completely suppressed in the 2.2%-Zn-doped samples at  $x = 0.66$ , in which we can measure the normal-state transport properties down to very low temperatures. Incidentally, the low-temperature normal-state transport has already been measured for pristine BSLCO crystals with  $x = 0.66$  under 60-T magnetic field,<sup>12</sup> so we can directly compare the normal state brought about by Zn-doping to that brought about by high magnetic fields. As is shown in Fig. 3(a),<sup>15</sup>  $\rho_{ab}(T)$  increases with decreasing temperature below  $\sim 30$  K and the temperature dependence is quicker than  $\log(1/T)$ , which is inferred from a positive curvature in this semi-log plot; this behavior is contrasting to the “metallic” behavior found<sup>12</sup> in the pristine sample with  $x = 0.66$ , where  $\rho_{ab}$  becomes temperature independent below  $\sim 10$  K with  $\rho_{ab} \simeq 190 \mu\Omega\text{cm}$ . Therefore, the localization behavior in the Zn-doped sample is clearly due to the additional scattering caused by the Zn impurities. Also, since the “insulating” behavior found<sup>12</sup> in more underdoped pristine samples ( $p < 1/8$ ) is consistent with  $\log(1/T)$  (which is slower than the behavior of the Zn-doped samples), the nature of the charge-localized

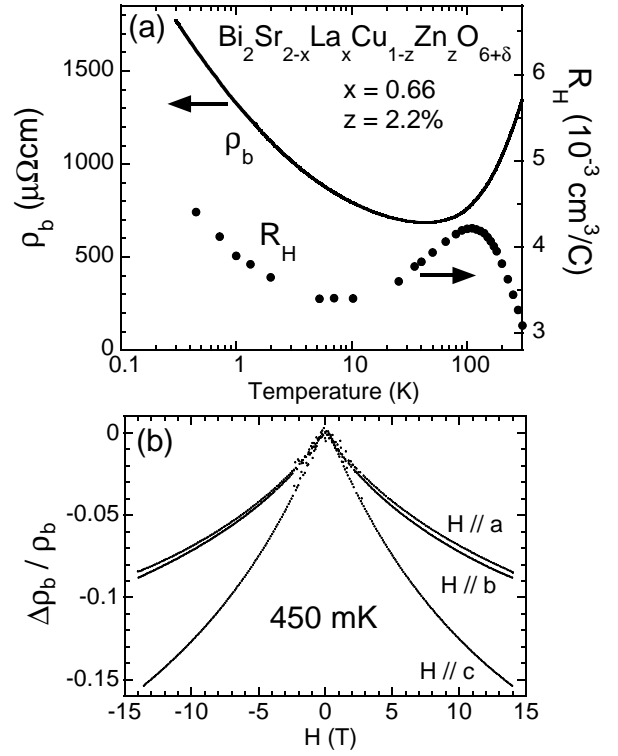


FIG. 3. (a)  $\log T$  plot of  $\rho_b$  of a 2.2%-Zn-doped  $x = 0.66$  sample;  $R_H(T)$  is also plotted using the right-hand-side axis. (b) Magnetoresistance of the above  $\rho_b$ -sample ( $I \parallel b$ ) at 450 mK for  $H$  along  $a$ ,  $b$ , and  $c$ .

state in the Zn-doped sample is apparently different from that in the pristine sample under high magnetic field.

It is found that  $R_H$  of the non-superconducting Zn-doped samples also shows an upturn at low temperatures [Fig. 3(a)]; this is again in contrast to the  $R_H(T)$  behavior of the pristine samples<sup>16</sup> under 60 T, which becomes essentially temperature independent at low temperatures. The rather strong temperature dependence of  $R_H$  below  $\sim 3$  K in the Zn-doped samples strongly suggests that the Zn-induced charge localization is *not* due to a simple weak localization effect.<sup>16</sup>

We can obtain further insight into the Zn-induced localized state from the magnetoresistance (MR), which turns out to be negative at low temperatures and is very peculiar. Figure 3(b) shows the MR at 450 mK for three geometries; the sample was cut so that the current  $I$  flows along the  $b$ -axis, and the magnetic field  $H$  is applied along  $a$ ,  $b$  (longitudinal geometry), and  $c$  (transverse geometry). There is essentially no anisotropy between  $H \parallel a$  and  $H \parallel b$ . The anisotropy between  $H \parallel b$  and  $H \parallel c$  is less than a factor of 2 and the  $H$  dependences for the two geometries are almost exactly the same. Therefore, we can conclude that the MR is essentially isotropic and thus is of spin origin. The  $H$  dependence of this negative MR is not  $H^2$  but is reminiscent of the  $H$  dependence expected for Kondo scattering.<sup>17–19</sup> Since the Kondo effect should yield isotropic MR, the main features of the

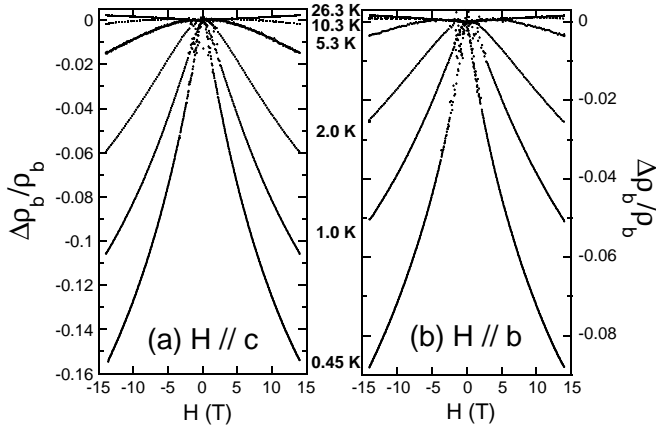


FIG. 4. Magnetoresistance of a 2.2%-Zn-doped  $x = 0.66$  sample for (a)  $H \parallel c$  (transverse) and (b)  $H \parallel b$  (longitudinal) at low temperatures ( $I \parallel b$ ).

MR observed here appears to be consistent, at least qualitatively, with what is expected for the Kondo effect. It is useful to note that a very anisotropic negative MR coming from weak localization has been observed<sup>20</sup> in non-superconducting samples of pristine  $\text{Bi}_2\text{Sr}_2\text{CuO}_{6+\delta}$ , which is contrasting to our observation in the Zn-doped samples.

The evolution of the MR with temperature is shown in Fig. 4 for  $H \parallel c$  and  $H \parallel b$ . The MR becomes predominantly negative below  $\sim 5$  K, which is nearly the same as the onset temperature of the low-temperature upturn in  $R_H(T)$ , and therefore the negative MR and the increase in  $R_H$  appear to have a common origin. It is useful to note that the Kondo scattering is expected to become effective simultaneously in the MR and in the Hall effect.<sup>19</sup> Thus, all the above results of the low-temperature MR and  $R_H$  seem to be most consistent with the Kondo effect, which may be caused<sup>6,21</sup> by the local moments<sup>7</sup> induced by the Zn impurities. The possibility that the Kondo effect is playing a major role in the Zn-doped samples also explains the various differences between the normal state in the Zn-doped samples and that in pristine samples under high magnetic fields. For more quantitative understanding of the possible Kondo effect in the cuprates, theoretical calculations for the Kondo scattering in the non-Fermi-liquid ground state of the cuprates would be required.

To summarize, in the BSLCO crystals we observed quite typical Zn-doping effects on  $\rho_{ab}(T)$  and  $\cot \theta_H(T)$ , and found no 1/8 anomaly in the  $T_c$  suppression rate. Comparison of the low-temperature normal state brought about by Zn-doping to that brought about by high magnetic field reveals significant difference between the two, which highlights the peculiar nature of the charge-localized state in the Zn-doped samples. The negative MR and the upturn in  $R_H$  observed at low temperatures strongly suggest that the Kondo scattering due to the local moments induced by Zn is playing a key role.

We thank S. Uchida and A. N. Lavrov for helpful dis-

cussions and T. Murayama for technical assistance.

\* Present address: Mitsubishi Gas Chemical Company, Inc., Katsushika-ku, Tokyo 125-0051, Japan.

† Corresponding author. E-mail: ando@criepi.denken.or.jp.

- <sup>1</sup> Y. Ando and T. Murayama, Phys. Rev. B **60**, R6991 (1999).
- <sup>2</sup> Y. Ando, Y. Hanaki, S. Ono, T. Murayama, K. Segawa, N. Miyamoto, and S. Komiya, Phys. Rev. B **61**, R14956 (2000); **63** 069902(E) (2001).
- <sup>3</sup> T.R. Chien, Z.Z. Wang, and N.P. Ong, Phys. Rev. Lett. **67**, 2088 (1991).
- <sup>4</sup> Y. Fukuzumi, K. Mizuhashi, K. Takenaka, and S. Uchida, Phys. Rev. Lett. **76**, 684 (1996).
- <sup>5</sup> K. Segawa and Y. Ando, Phys. Rev. B **59**, R3948 (1999).
- <sup>6</sup> N. Nagaosa and P. A. Lee, Phys. Rev. Lett. **79**, 3755 (1997).
- <sup>7</sup> H. Alloul, P. Mendels, H. Casalta, J.-F. Marucco, and J. Arabski, Phys. Rev. Lett. **67**, 3140 (1991).
- <sup>8</sup> Y. Koike, S. Takeuchi, Y. Hama, H. Sato, T. Adachi, and M. Kato, Physica C **282-287**, 1233 (1997).
- <sup>9</sup> M. Akoshima, T. Noji, Y. Ono, and Y. Koike, Phys. Rev. B **57**, 7491 (1998).
- <sup>10</sup> K. Hirota, K. Yamada, I. Tanaka, and H. Kojima, Physica B **241-243**, 817 (1998).
- <sup>11</sup> J. M. Tranquada, B. J. Sternlieb, J. D. Axe, Y. Nakamura, and S. Uchida, Nature **375**, 561 (1995).
- <sup>12</sup> S. Ono, Y. Ando, T. Murayama, F. F. Balakirev, J. B. Betts, and G. S. Boebinger, Phys. Rev. Lett. **85**, 638 (2000).
- <sup>13</sup> K. Mizuhashi, K. Takenaka, Y. Fukuzumi, and S. Uchida, Phys. Rev. B **52**, R3884 (1995).
- <sup>14</sup> This observation is actually in good accord with the M-I crossover<sup>12</sup> occurring at  $p \simeq 1/8$  in pristine BSLCO, because such M-I crossover could mean that the static stripes (which presumably cause charge localization in the normal state) disappear above  $p \simeq 1/8$  in BSLCO.
- <sup>15</sup> The sample measured for Fig. 3(a) is different from that for Fig. 1(b). We have measured more than 10 samples from the same batch of  $(x, z) = (0.66, 0.022)$ , and found that the resistivity values at 300 K differ by up to 20%, which is presumably due to slight differences in the Zn concentration. The low-temperature localization behavior is found to be correspondingly different, becoming stronger as  $\rho_{ab}$  at 300 K becomes larger. However, the MR behavior is essentially reproducible in all the samples measured.
- <sup>16</sup> Y. Ando, G.S. Boebinger, A. Passner, N. L. Wang, C. Geibel, F. Steglich, I. E. Tofimov, and F. F. Balakirev, Phys. Rev. B **56**, R8530 (1997).
- <sup>17</sup> N. Andrei, K. Furuya, and J. H. Lowenstein, Rev. Mod. Phys. **55**, 331 (1983).
- <sup>18</sup> P. Schlottmann, Phys. Rep. **181**, 1 (1989).
- <sup>19</sup> J. Ruvalds and Q. G. Sheng, Phys. Rev. B **37**, 1959 (1988).
- <sup>20</sup> T. W. Jing, N. P. Ong, T. V. Ramakrishnan, J. M. Tarascon, and K. Remschnig, Phys. Rev. Lett. **67**, 761 (1991).
- <sup>21</sup> J. Bobroff, W. A. MacFarlane, H. Alloul, P. Mendels, N. Blanchard, G. Collin, and J.-F. Marucco, Phys. Rev. Lett. **83**, 4381 (1999).